Phosphorane intermediate *vs.* leaving group stabilization by intramolecular hydrogen bonding in the cleavage of trinucleoside monophosphates: implications for understanding catalysis by the large ribozymes†

Tuomas Lönnberg* and Maarit Laine

Received 19th June 2009, Accepted 13th October 2009
First published as an Advance Article on the web 19th November 2009
DOI: 10.1039/b912042d

Hydrolysis of 2′,3′-*O*-methyleneadenosin-5′-yl 5′-*O*-methyluridin-2′-yl 5′-*O*-methyl-2′-trifluoroacetamido-2′-deoxyuridin-3′-yl phosphate (**1b**) has been followed by HPLC over a wide pH range to study the effects of potential hydrogen bonding interactions of the 2′-trifluoroacetamido function on the rate and product distribution of the reaction. At pH < 2, decomposition of **1b** (and its 3′,3′,5′-isomer **1a**) is first-order in hydronium-ion concentration and cleavage of the P–O3′ bond of the 2′-trifluoroacetamido-modified nucleoside is slightly favored over cleavage of the P–O5′ bond. Between pH 2 and 4, the overall hydrolysis is pH-independent and the P–O3′ and P–O5′ bonds are cleaved at comparable rates. At pH 5, the reaction becomes first-order in hydroxide-ion concentration, with P–O3′ bond cleavage predominating. At 10 mmol L^{-1} aqueous sodium hydroxide, no P–O5′ bond cleavage is observed. Compared to the 2′-OH counterpart **2**, a modest rate enhancement is observed over the entire pH range studied. The absence of P–O5′ fission under alkaline conditions suggests hydrogen bond stabilization of the departing 3′-oxyanion by the neighboring 2′-trifluoroacetamido function.

Introduction

Although the transesterification reactions catalyzed by group I introns are initiated by an external nucleophile, rather than the intramolecular 2′-hydroxy group flanking the scissile phosphodiester linkage, the latter is nevertheless essential for the catalytic efficiency of these ribozymes.[1,2] In other words, DNA is not a substrate for group I introns. It has been proposed on the basis of studies with modified group I ribozymes that the 2′-OH stabilizes the departing 3′-oxyanion by donating a hydrogen bond.[1–3] Effects of 2′-substitution on the rate of hydrolysis and isomerization of related trinucleoside 3′,3′,5′-monophoshates and -phosphorothioates, on the other hand, are best explained in terms of hydrogen bonding between the 2′-OH and the non-bridging phosphoryl oxygen.[4–6] With both phosphotriester and phosphorothioate models, the 2′-OH group of the 3′-linked departing nucleoside considerably accelerates hydrolysis relative to the 2′-OMe counterparts but the effect is equal on P–O5′ and P–O3′ bond fission (Scheme 1, Routes A and B, respectively). Isomerization is facilitated by the 2′-OH function as well, although the effect could only be quantified in the case of the phosphotriester models. In particular, the latter observation strongly suggests stabilization of the phosphorane intermediate common to both cleavage and isomerization pathways.

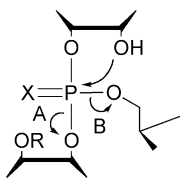

X = O or S
R = H or Me

Scheme 1 Cleavage of a trinucleoside monophosphate or phosphorothioate *via* P–O5′ (Route A) or P–O3′ (Route B) fission.

The 2′-hydroxy function of the departing 3′-linked nucleoside has been suggested to participate in a hydrogen-bonding network which serves to increase its acidity and orient it favorably for hydrogen bonding with the developing 3′-oxyanion.[7–10] Several examples of perturbed pK_a values in various ribozyme structures have been reported.[11] Duplication of the latter effect in a small molecular model is challenging but the former may be achieved by replacing the 2′-OH with a more acidic group. To this end, a trinucleoside 2′,3′,5′-monophosphate model (**1b**) having the 2′-hydroxy function of the 3′-linked nucleoside replaced with a trifluoroacetamido group has been prepared and its hydrolysis followed over a wide pH range. *N*-Alkyltrifluoroacetamides are approximately 2 orders of magnitude more acidic than corresponding alcohols so **1a** and **1b** are expected to hydrolyze significantly faster than the 2′-hydroxy counterpart **2** (or the 2′-OMe counterpart **3**). Furthermore, comparison of the relative rates of P–O5′ (Route A) and P–O3′ (Route B) fission under alkaline conditions, where the leaving group departs as an oxyanion, allows one to differentiate between the two possible modes of acceleration (relative to the 2′-OMe analogue **3**). If hydrogen bond stabilization of the departing 3′-oxyanion by the neighboring 2′-hydroxy group plays

Department of Chemistry, University of Turku, FIN-20014, Turku, Finland. E-mail: tuanlo@utu.fi; Fax: +358 2 333 6700; Tel: +358 2 333 6777

† Electronic supplementary information (ESI) available: NMR and UV spectra and HPLC chromatograms of compounds **11**, **7** and **4b**, NMR spectra of compounds **10** and **5b**, observed pseudo first-order rate constants and product distributions for the hydrolysis of **1a** and **1b** and a sample chromatogram of the RP HPLC analysis of the reaction mixtures. See DOI: 10.1039/b912042d

a major role in rate acceleration, then cleavage of the P–O3′ bond should be favored more with **1a** and **1b** than with the 2′-OMe analogue **3** (please note that similar acceleration of the P–O5′ cleavage is unlikely, as the putative stabilizing hydrogen bond must be broken before release of the 5′-oxyanion). Hydrogen bond stabilization of the phosphorane intermediate, on the other hand, should equally facilitate both cleavage reactions (Routes A and B).

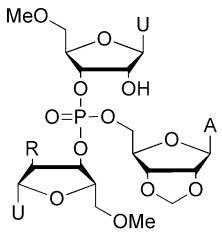

1a: R = NHTfa
2 : R = OH
3 : R = OMe

Results and discussion

Preparation of the model trinucleoside monophosphate (4b)

N^6-Benzoyl-2′,3′-*O*-methyleneadenosin-5′-yl 5′-*O*-methyl-3′-*O*-(4,4′-dimethoxytrityl)uridin-2′-yl 5′-*O*-methyl-2′-trifluoroacetamido-2′-deoxyuridin-3′-yl phosphate (**5b**) was obtained by tetrazole-promoted stepwise displacement of the dimethylamino groups from tris(dimethylamino)phosphine with the appropriately protected nucleosides (**6**, **7** and **8**) (Scheme 2). The nucleosides, in turn, were prepared by applying procedures described in the literature.[6,12,13] Removal of the N^6-benzoyl protection with methanolic ammonia, followed by RP HPLC purification, afforded the desired phosphotriester **4b** as a single diastereomer (the absolute configuration at phosphorus was not determined), as evidenced by detection of only one signal in ^{31}P NMR, signals arising from only one compound in ^{1}H NMR and also only a single peak in RP HPLC. According to our previous experience, R_P- and S_P-diastereomers of trinucleoside monophosphates and phosphorothioates yield two peaks in ^{31}P NMR and two sets of peaks in ^{1}H NMR and are separable by RP HPLC.[6] It is also worth pointing out that in the N^6-position of the adenine base, benzoyl protection is labile enough to be removed leaving the 2′-*N*-trifluoroacetyl group as well as the phosphotriester linkage intact.

Product distribution and reaction pathways

The hydrolytic reactions of **1b** were followed over a wide pH range (from H_0 = –0.1 to pH = 6.73) at 25 °C by analyzing the composition of aliquots withdrawn from the reaction mixture at appropriate time intervals by RP HPLC. First, the 3′-*O*-(4,4′-dimethoxytrityl) protection of **4b** was removed with 0.10 mol L^{-1} HCl in 1,4-dioxane to give **1b**. An appropriate prethermostated aqueous solution was then immediately added to yield the desired reaction solution so that the final dioxane content was 5% (v/v). The aliquots were quenched by cooling to –16 °C and adjusting their pH to *ca.* 3.5 with formic acid or sodium formate when necessary. The products were characterized either by spiking with authentic samples or by mass spectrometric analysis (HPLC/ESI$^-$-MS). The peak areas were converted to relative concentrations by calibrating the system with uridine and adenosine solutions of known concentration.

Two sets of products formed by two distinct routes were observed over the entire pH range (Scheme 3). Cleavage of the P–O5′ bond (Route A) yields 2′,3′-*O*-methyleneadenosine (**15**) and the isomeric diesters 5′-*O*-methyluridylyl-3′,3′-(5′-*O*-methyl-2′-trifluoroacetamido-2′-deoxyuridine) (**16a**) and 5′-*O*-methyluridylyl-2′,3′-(5′-*O*-methyl-2′-trifluoroacetamido-2′-deoxyuridine) (**16b**). Cleavage of the P–O3′ bond (Route B), in turn, gives 5′-*O*-methyl-2′-trifluoroacetamido-2′-deoxyuridine (**7**) accompanied by the isomeric diesters 5′-*O*-methyluridylyl-3′,5′-(2′,3′-*O*-methyleneadenosine (**17a**) and 5′-*O*-methyluridylyl-2′,5′-(2′,3′-*O*-methyleneadenosine (**17b**). At pH < 4, cleavage of the P–O5′ and P–O3′ proceed at comparable rates, while under more alkaline conditions cleavage of the P–O3′ bond is significantly faster.

The pseudo first-order rate constants for the disappearance of **1a** and **1b** were obtained by applying the integrated first-order rate equation to the time-dependent diminution of the peak area of the starting material. Significant buffer catalysis was observed with the carboxylate buffers. In these cases, buffer-independent rate constants were obtained by varying the buffer concentration from 0.0475 to 0.190 mol L^{-1} and extrapolating the observed pseudo first-order rate constants to zero buffer concentration by linear regression.

pH–Rate profiles

The pH–rate profile for the overall disappearance of **1** is presented in Fig. 1. At pH < 2, the overall reaction is first order in [H_3O^+] and cleavage of the P–O3′ bond (Route B) is slightly favored over cleavage of the P–O5′ bond (Route A), accounting for 69% of the overall hydrolysis. Between pH 2 and 4, the overall reaction is pH-independent with comparable contributions from both routes. At pH > 4, the overall reaction becomes first-order in [HO^-] and P–O3′ bond fission starts to dominate again (Fig. 2). In 10 mmol L^{-1} aq. NaOH, no P–O5′ bond cleavage is observed.

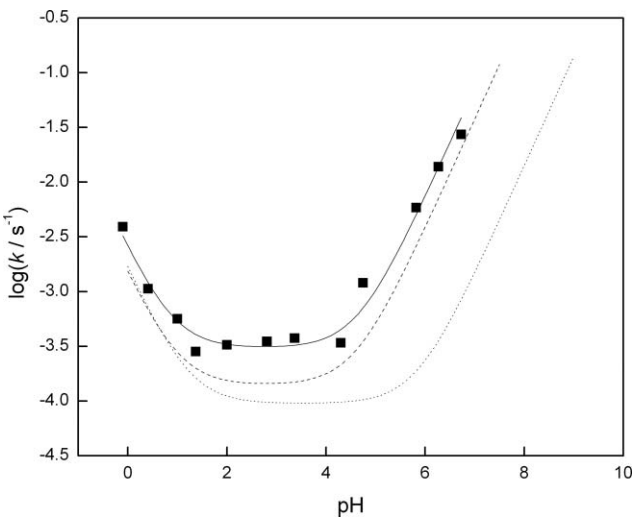

Fig. 1 pH–Rate profile for the cleavage of **1a** and **1b** (■), **2** (dashed line) and **3** (dotted line) at 25.0 °C, I(NaNO$_3$) = 1.0 mol L^{-1}.

Mutual isomerization between **1a** and **1b** is rapid and an equilibrium is already settled during the deprotection of the precursor **4b**,

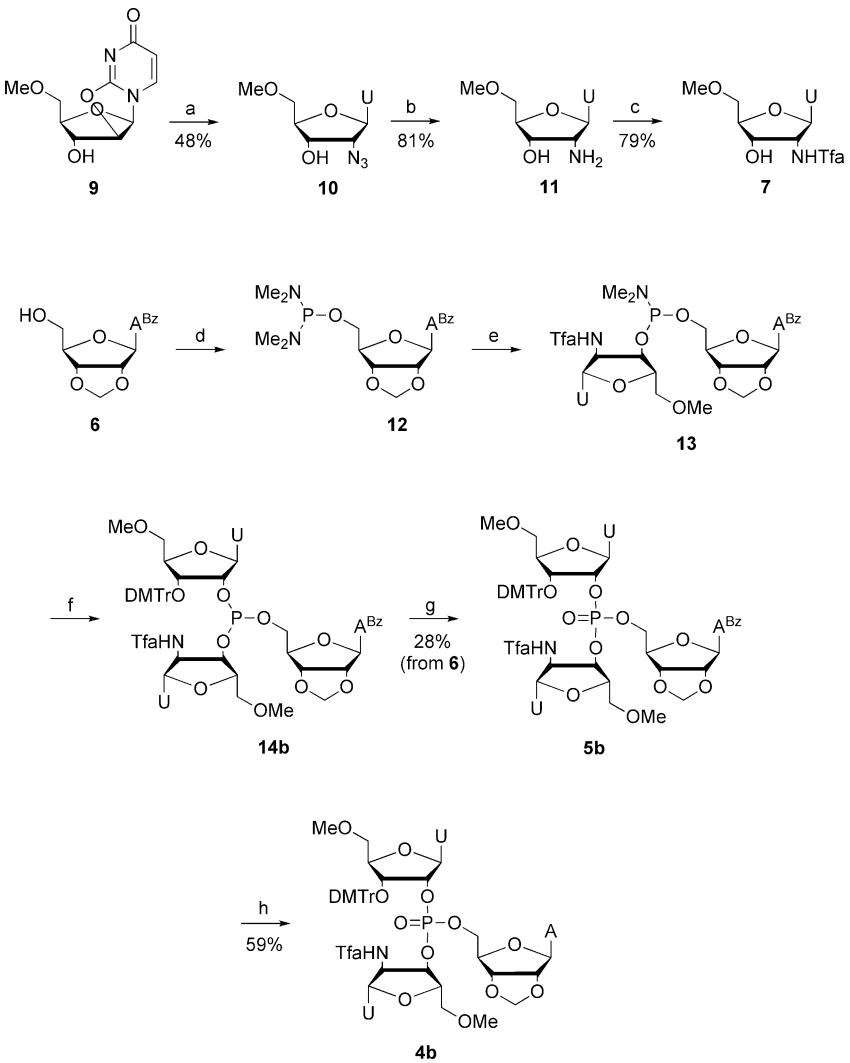

Scheme 2 Preparation of the trinucleoside 2′,3′,5′-monophosphate **4b**. *Reagents and conditions*: (a) NaN_3, DMF, (b) (1) Ph_3P, pyridine, (2) aq. NH_3, pyridine, (c) *S*-ethyltrifluorothioacetate, MeOH, (d) $(Me_2N)_3P$, 1*H*-tetrazole, MeCN, (e) **7**, 1*H*-tetrazole, MeCN, (f) 5′-*O*-methyl-3′-*O*-(4,4′-dimethoxytrityl)uridine, 1*H*-tetrazole, MeCN, (g) I_2, THF, H_2O, 2,6-lutidine, (h) NH_3, MeOH.

preventing kinetic analysis of this reaction. Qualitatively, however, the observation is in line with previous results on similar nucleoside phosphotriesters. For example, with both 5′-*O*-pivaloyluridine 3′-dimethylphosphate[14] as well as the more elaborate trinucleoside monophosphate model **2**,[6] isomerization becomes first-order in [HO^-] already at pH 2 and is 10^5 times as rapid as cleavage under alkaline conditions. Under acidic conditions, the difference is less marked but with compound **2**, isomerization is still *ca.* 4 times as rapid as cleavage. As previously reported for phosphoromonothioate analogs of uridylyl(3′,5′)uridine, migration of the phosphate from 2′- to 3′-position proceeds with retention of configuration at phosphorus.[15]

Between pH 3 and 5, *i.e.* when the reactions are carried out in carboxylate buffers, considerable buffer catalysis is observed. The sole catalytically active species is the basic buffer constituent, *viz.* the carboxylate anion. The second-order rate constants for the catalysis by formic and acetic acid buffers at different ratios of [HA] to [A^-] are summarized in Table 1.

The observed pseudo first-order rate constant for the overall cleavage of **1**, k_{cl}^{obs}, may be expressed by eqn (1).

$$k_{cl}^{obs} = k_{cl}^{H} a_{H^+} + k_{cl}^{W} + \frac{k_{cl}^{OH} K_W}{a_{H^+}} \quad (1)$$

a_{H^+} is hydronium ion activity, k_{cl}^{H}, k_{cl}^{W} and k_{cl}^{OH} are the rate constants for the hydronium ion catalyzed, pH-independent and hydroxide ion catalyzed cleavage, respectively and $K_W = 1.875 \times 10^{-14}$ mol L^{-1} is the ion product of water under the experimental conditions.[16] The rate constants were obtained by nonlinear least-squares fitting of the experimental values to eqn (1). On the basis of the relative concentrations of the monomeric products of the two competing reaction pathways (**15** and **7** for Routes A and B, respectively), the rate constants of the overall cleavage of **1a** and **1b**, k_{cl}, may then be broken down into the rate constants for the partial reactions, *viz.* cleavage of the P–O5′ (Route A) and P–O3′ (Route B) bonds [eqn (2) and (3)]. The rate constants thus obtained

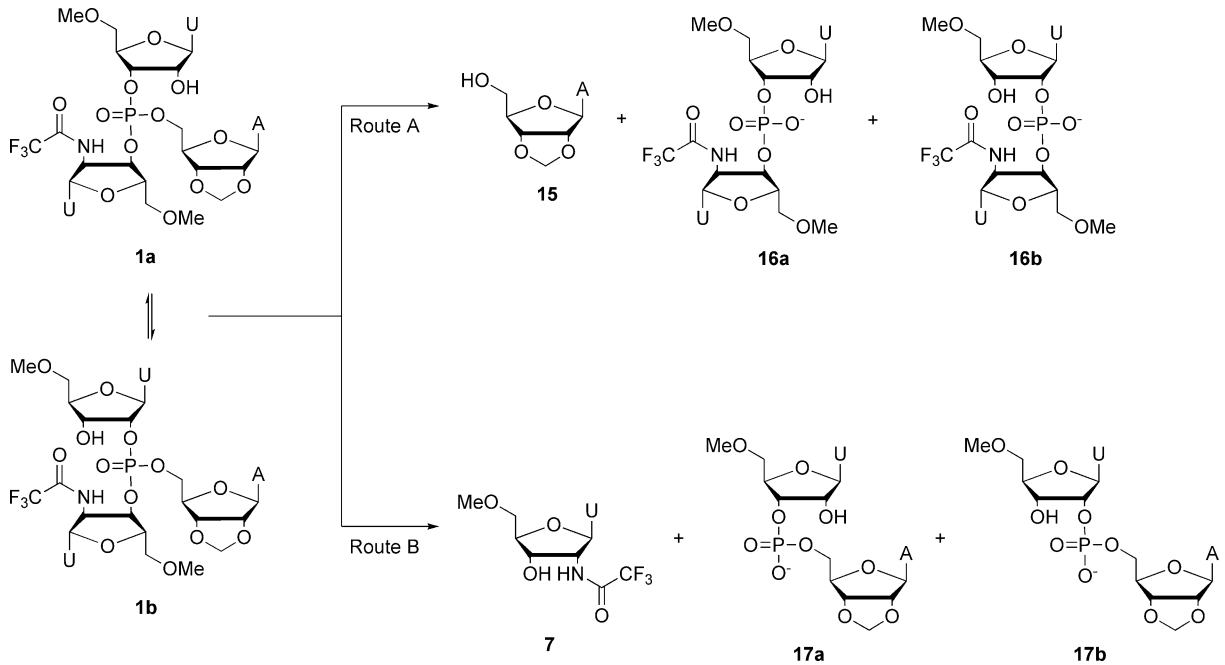

Scheme 3 Hydrolytic reaction pathways of **1a** and **1b**.

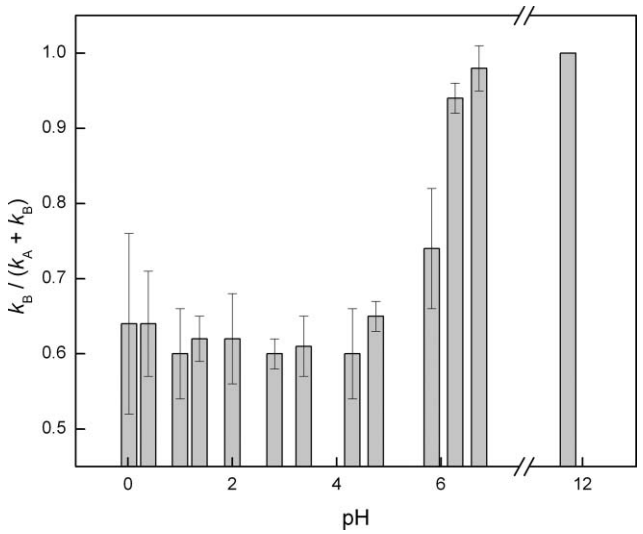

Fig. 2 Ratio of k_B (Route B) to $k_{cl} = k_A + k_B$ (overall cleavage) of **1a** and **1b** as a function of pH at 25.0 °C, $I(NaNO_3) = 1.0$ mol L^{-1}.

Table 1 Rate constants for the buffer-catalyzed cleavage of **1a** and **1b** ($T = 25.0$ °C, $I(NaNO_3) = 1.0$ mol L^{-1})

Buffer	$[A^-]/[HA]$	[buffer]/ mmol L^{-1}	$k_{obs}/10^{-4}$ s^{-1}	$k_{cl}^{buf}/10^{-3}$ L mol^{-1}s^{-1}
Formate (pH 2.81)	3 : 17	47.5	4.34	
		95.0	5.18	
		190.0	7.24	
				2.1 ± 0.1
Formate (pH 3.37)	2 : 3	47.5	6.18	
		95.0	8.03	
		142.5	9.51	
		190.0	12.9	
				4.6 ± 0.6
Acetate (pH 4.30)	2 : 3	47.5	14.4	
		95.0	22.4	
		142.5	35.9	
		190.0	44.4	
				22 ± 2
Acetate (pH 4.75)	13 : 7	47.5	23.7	
		95.0	35.6	
		142.5	44.9	
		190	58.9	
				24 ± 1

are presented in Table 2, along with those previously obtained for **2** and **3**.

$$k_A = \frac{[\mathbf{7}]}{[\mathbf{15}]+[\mathbf{7}]} k_{cl} \quad (2)$$

$$k_B = \frac{[\mathbf{15}]}{[\mathbf{15}]+[\mathbf{7}]} k_{cl} \quad (3)$$

Estimation of the pK_a values of the leaving groups

The pK_a values of the secondary hydroxy functions of adenosine and 2′-*O*-methyladenosine have been determined by ^{13}C NMR titrations as 12.79 and 13.53, respectively.[17] Assuming that the acidity of the sugar hydroxy groups does not significantly depend on the identity of the base moiety, these values represent a good estimation of the pK_a values of the 3′-linked leaving groups of **2** and **3** (5′-*O*-methyluridine and 2′,5′-di-*O*-methyluridine), respectively. Furthermore, a good linear correlation between the acidities of the 3′-OH and the electronegativity of the 2′-substituent (Mullay's improved group electronegativities[18] or Inamoto's ι values[19]) was reported, allowing estimation of the acidity of the 3′-OH of the 2′-trifluoroacetamido analog **7**. Based on Inamoto's ι values, pK_a(**7**) = 13.57. On the basis of kinetic data, we have previously estimated the 5′-hydroxy function of 2′,3′-*O*-methyleneadenosine (**15**) to be approximately one order of magnitude less acidic than

Table 2 Rate constants for the partial reactions of the cleavage of **1a**, **b**, **2** and **3** ($T = 25.0$ °C, $I(NaNO_3) = 1.0$ mol L^{-1})

		$k^H/10^{-3}$ L mol^{-1} s^{-1}	$k^W/10^{-4}$ s^{-1}	$k^{OH}/10^5$ L mol^{-1} s^{-1}
1a, **b**	k_{cl}	2.3 ± 0.5	3.0 ± 0.4	3.8 ± 0.6
	k_B	1.5 ± 0.3	1.8 ± 2	3.8 ± 0.6
	k_A	0.8 ± 0.2	1.2 ± 2	0[a]
2	k_{cl}	1.4 ± 0.1	1.4 ± 0.2	2.0 ± 0.1
	k_B	0.70 ± 0.05	0.5 ± 0.1	1.78 ± 0.09
	k_A	0.70 ± 0.05	0.9 ± 0.1	0.22 ± 0.01
3	k_{cl}	1.6 ± 0.3	0.9 ± 0.09	0.075 ± 0.009
	k_B	0.6 ± 0.1	0.23 ± 0.02	0.066 ± 0.008
	k_A	1.0 ± 0.2	0.68 ± 0.07	0.009 ± 0.001

[a] Could not be determined due to overwhelming predominance of the competing P–O3′ cleavage (Route B).

the 3′-hydroxy function of 2′,5′-di-*O*-methyluridine, *i.e.* pK_a(**15**) = 14.5.[12]

Hydronium-ion catalyzed cleavage

At pH < 2, the overall disappearance of **1a** and **1b** is first-order in [H_3O^+]. The hydronium-ion catalyzed hydrolysis of **1a** and **1b** is 1.7 times as rapid as the corresponding reaction of the 2′-OH and 2′-OMe analogues (**2** and **3**, respectively), fission of the P–O3′ bond (Route B) accounting for two thirds of the overall cleavage. In other words, P–O5′ cleavage (Route A) is equally rapid with all models, whereas departure of a 3′-linked nucleoside containing a 2′-trifluoroacatamido group is twice as fast as departure of the 2′-OH and 2′-OMe counterparts. Because the leaving groups depart as alcohols (Scheme 4), the rate of the reaction is only modestly sensitive to the acidity of the leaving group, the β_{lg} value previously reported for ribonucleoside 3′-(alkyl isopropyl phosphates) being –0.40.[20] The $k_B{}^H/k_A{}^H$ ratio expected on the basis of the β_{lg} value and the estimated difference of 0.7 between the pK_a values of **7** and **15** is 1.9, in excellent agreement with the observed ratio of 2. Consistent with previous results on methyl ethylene phosphate, the initial cyclic phosphotriester products resulting from the release of the nucleosides **7** and **15** do not accumulate but are rapidly converted to the more stable phosphodiester products **17a**, **b** and **16a**, **b** by attack of water on the phosphorus.[21] No nucleoside monophosphate products are detected either, suggesting that cleavage proceeds essentially exclusively *via* cleavage of one of the endocyclic P–O bonds. In fact, some controversy still exists as to whether or not exocyclic P–O bond cleavage takes place at all.[21]

Hydroxide-ion catalyzed cleavage

At pH > 4, the overall disappearance of **1a**, **b** is first-order in [HO^-]. On going to more alkaline conditions, cleavage of the P–O3′ bond (Route B) becomes more and more favored until, in 10 mmol L^{-1}, no P–O5′ cleavage (Route A) can be detected. The base-catalyzed cleavage proceeds by departure of an alkoxide ion (Scheme 5), making the reaction highly sensitive to the pK_a of the leaving group, so a change in product distribution to favor Route B is expected. However, based on the estimated pK_a difference between **7** and **15** and the previously reported β_{lg} value of –1.38,[20] a 4% contribution by Route A would still be expected. The observation of exclusive P–O3′ cleavage is also in contrast with the results on the base-catalyzed hydrolysis of **2** and **3**, where P–O5′ fission accounts for more than 10% of the overall reaction

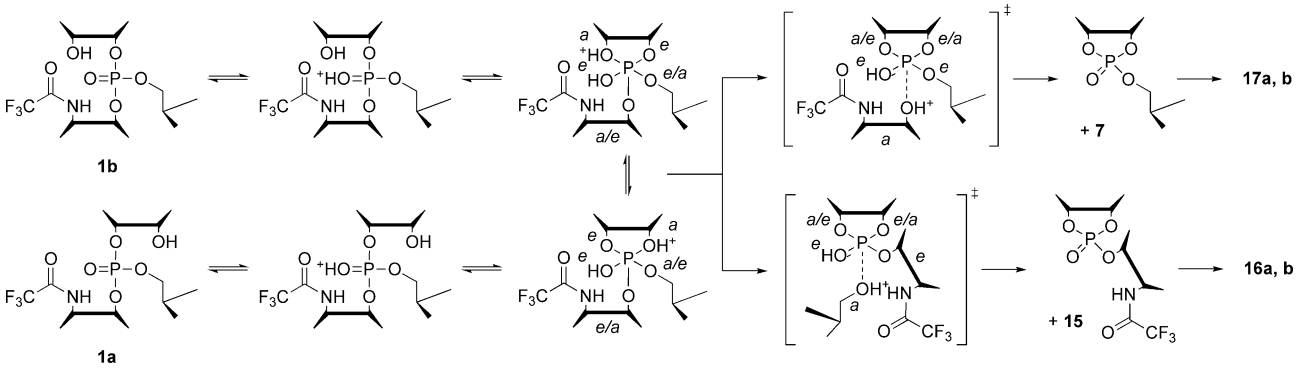

Scheme 4 Hydronium-ion catalyzed cleavage of **1a** and **1b**.

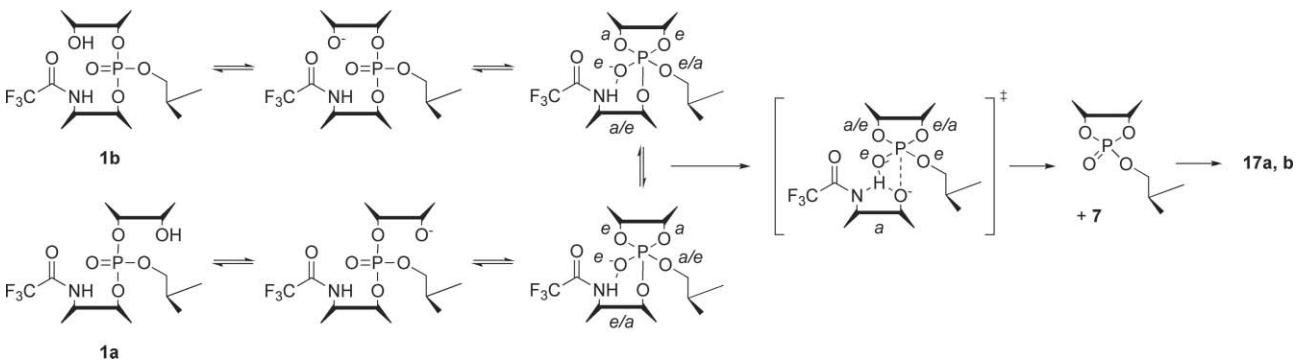

Scheme 5 Hydroxide-ion catalyzed cleavage of **1a** and **1b**.

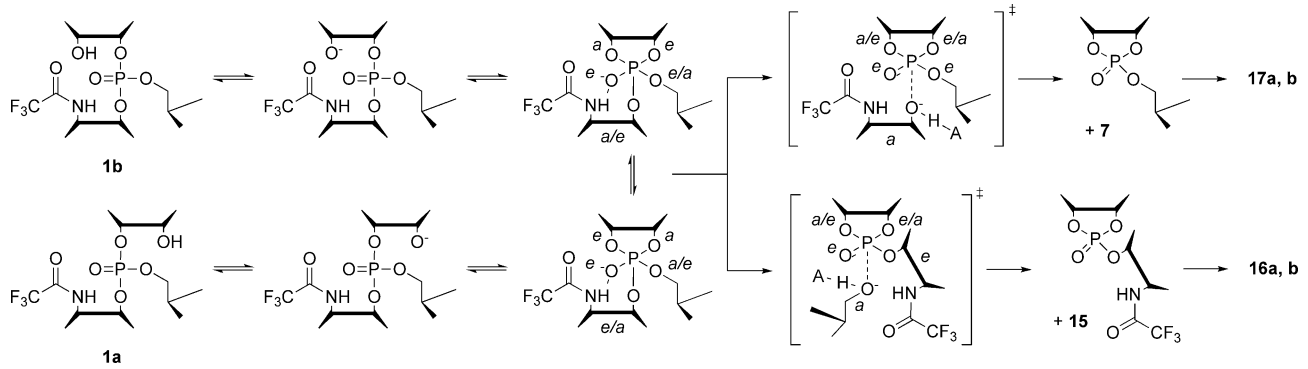

Scheme 6 pH-Independent buffer catalyzed cleavage of **1a** and **1b**.

even under highly alkaline conditions. The apparent discrepancy may be taken as evidence for hydrogen bond stabilization of the departing 3′-oxyanion by the 2′-trifluoroacetamido function. This interpretation receives additional support from semiempirical MOPAC (PM6)[22] modeling of the monoanionic phosphorane intermediates of the base-catalyzed cleavage of **1** and **2**: the 2′-hydroxy group of **2** donates a hydrogen bond to the non-bridging phosphorane oxygen, whereas the 2′-trifluoroacetamido group of **1** forms a bifurcated hydrogen bond with the developing 3′-oxyanion and the non-bridging oxygen (Fig. 3). Thus, even though the 3′-oxyanion of **7** is inherently a poorer leaving group than the 3′-oxyanion of 5′-*O*-methyluridine, it nevertheless departs more readily under alkaline conditions. Overall, rate acceleration by the 2′-trifluoroacetamido group relative to the 2′-OH group is rather modest: the second-order rate constants for the hydroxide-ion catalyzed cleavage of **1**, **2** and **3** are 380, 200 and 7.5×10^3 L mol^{-1} s^{-1}, respectively. As described above for the hydronium-ion catalyzed cleavage, the immediate cyclic phosphotriester products are rapidly hydrolyzed to the phosphodiester products **17a**, **b** and **16a**, **b** and, hence, are not detected. Furthermore, absence of any nucleoside monophosphate products indicates that only endocyclic P–O bond fission takes place.

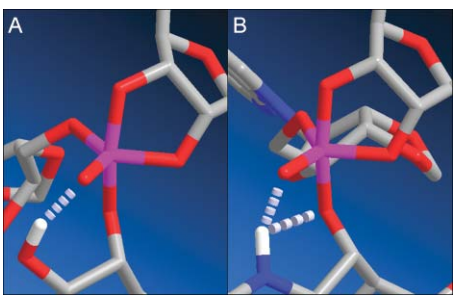

Fig. 3 PM6-minimized structures of the monoanionic phosphorane intermediates of the hydroxide-ion catalyzed cleavage and isomerization **2** (A) and **1a**, **b** (B). The hydrogen bonds donated by the 2′-substituent are depicted as white dashed bonds.

pH-Independent and buffer catalyzed cleavage

Between pH 2 and 4, the cleavage of **1a**, **b** is pH-independent but subject to general base catalysis by carboxylate anions. The observed buffer catalysis may be interpreted as a sequential specific base/general acid catalysis with the attacking 2′-OH being deprotonated in a preequilibrium step and proton transfer from the general acid to the departing oxyanion takes place concerted with the rate-limiting P–O bond fission (Scheme 6).[14] The second-order rate constants for the buffer catalyzed cleavage of the P–O3′ (Route B) and P–O5′ (Route A) bonds are largely equal, probably because the polar effects of the departing nucleoside on the rate of proton transfer and bond cleavage are opposite. The β_{lg} value previously reported for this reaction is –0.73.[20] The ratio of P–O3′ (Route B) to P–O5′ (Route A) fission for the pH- and buffer-independent reaction is 1.6, significantly higher than the values previously observed for **2** (0.64) and **3** (0.33). The Brønsted β value for the observed general base catalysis is approximately 0.7 which corresponds to an α value of 0.3 for the general acid catalysis. Together with the β_{lg} value of –0.73 and the previously reported β_{eq} value of –1.83,[23] these data indicate that P–O bond cleavage and proton transfer from the general acid to the departing oxygen are approximately equally advanced in the transition state. As described above for the hydronium-ion and hydroxide-ion catalyzed reactions, no cyclic phosphotriesters or nucleoside monophosphates resulting from their exocyclic P–O bond cleavage are detected.

Conclusions

The observation that the hydroxide-ion catalyzed cleavage of **1a** and **1b** proceeds exclusively *via* expulsion of the 2′-trifluoroacetamido-modified 3′-linked nucleoside suggests that the trifluoroacetamido function may stabilize the departing 3′-oxyanion by hydrogen bonding. This interpretation is also borne out by results of semiempirical molecular modeling of the monoanionic phosphorane intermediate of the reaction. The origin of this difference in behavior compared to the 2′-OH analogue **2** remains unclear, although one might speculate that the relatively bulky trifluoroacetamido group forces **1a** and **1b** to a conformation where the 2′-NH proton is oriented favorably for hydrogen bonding with the 3′-oxygen, rather than the non-bridging phosphoryl oxygen. This could also explain why **1a** and **1b** are hydrolyzed only approximately 2 times as fast as **2** even though the 2′-trifluoroacetamido group is 2 orders of magnitude more acidic than the 2′-hydroxy group possessing, hence, a much greater potential for accelerating the reaction by hydrogen bond stabilization of the phosphorane intermediate.

Experimental section

Materials

Nucleosides were commercial products and they were used as received after checking their purity by HPLC. The buffer constituents were of reagent grade.

Kinetic measurements

Reactions were carried out in sealed tubes immersed in a thermostated water bath, the temperature of which was adjusted to 25 °C within ± 0.1 °C. The reactions were started by adding the starting material in DMSO (5 μL) to 80 μL of 100 mmol L^{-1} HCl in 1,4-dioxane. After 30 min at 40 °C, 1520 μL of the desired reaction solution (prethermostated to 25 °C) was added. The hydronium ion concentration of the reaction solutions was adjusted with nitric acid and formate, acetate and MES buffers and checked with a pH meter. The ionic strength of the solutions was adjusted to 1.0 mol L^{-1} with $NaNO_3$. A significant buffer catalysis was observed with the carboxylate buffers. In these cases, buffer-independent rate constants were obtained by varying the buffer concentration from 0.0475 to 0.190 mol L^{-1} and extrapolating the observed pseudo first-order rate constants to zero buffer concentration by linear regression.

The initial substrate concentration in the kinetic runs was *ca.* 10^{-4} mol L^{-1}. The composition of the samples withdrawn at appropriate time intervals from the reaction mixture was analyzed by HPLC on a Hypersil-Keystone Aquasil C18 column (4 × 150 mm, 5 μm) using 0.06 mol L^{-1} formic acid buffer (pH = 3.0) and MeCN as an eluent. The amount of MeCN was linearly increased from 3% to 30% during 40 min. The observed retention times (t_R, min) with a flow rate of 1.0 mL min^{-1} for **1a**, **b** and its hydrolytic products were as follows: 32.7 (**1a**, **b**), 22.0, 21.4 (**16a**, **b**), 16.4, 15.0 (**17a**, **b**), 13.7 (**7**), 10.9 (**15**). The products were characterized either by spiking with authentic samples or by mass spectrometric analysis (HPLC/ESI-MS) and the peak areas were converted to relative concentrations by calibrating the system with uridine and adenosine solutions of known concentration. The pseudo first-order rate constants for the disappearance of **1a** and **1b** were obtained by applying the integrated first-order rate law to the time-dependent diminution of the peak area of the starting material. Isomerization of **1a** and **1b** was rapid and equilibrium between **1a** and **1b** had settled already in the first sample. Furthermore, compound **1b** decomposed somewhat during the deprotection and the product peaks for **15**, **16a**, **b**, **7** and **17a**, **b** were visible even in the first sample. To obtain the correct product distributions for the hydrolytic reactions, these initial concentrations were subtracted from the concentrations observed in the later samples.

Molecular modeling

Energy minimizations were performed by MOPAC2007 using the PM6 Hamiltonian, closed shell wave function, the EF optimizer and no solvent.[22]

5′-*O*-Methyl-2′-azido-2′-deoxyuridine (10)

5′-*O*-Methyl-2,2′-anhydro-1-β-*D*-arabinofuranosyluracil (**9**)[12] (3.34 g, 9.74 mmol) and NaN_3 (2.22 g, 34.1 mmol) were dissolved in DMF (23.75 mL). The mixture was stirred at 130 °C for 47 h, after which it was purified on a silica gel column eluting with a mixture of MeOH and CH_2Cl_2 (5 : 95, v/v). Yield 1.33 g (48%). ^{1}H NMR (δ_H)(500 MHz, DMSO-d_6): 11.45 (s, 1H), 7.69 (d, 1H, J = 8.2 Hz), 6.05 (d, 1H, J = 5.6 Hz), 5.83 (d, 1H, J = 5.2 Hz), 5.71 (d, 1H, J = 8.1 Hz), 4.28 (dd, 1H, J_1 = 10.8 Hz, J_2 = 5.4 Hz), 4.13 (dd, 1H, J_1 = 5.3 Hz, J_2 = 5.4 Hz), 3.97 (m, 1H), 3.60 (dd, 1H, J_1 = 11.0 Hz, J_2 = 3.1 Hz), 3.52 (dd, 1H, J_1 = 11.1 Hz, J_2 = 4.2 Hz), 3.33 (s, 3H). ^{13}C NMR (δ_H)(125 MHz, DMSO-d_6): 163.5, 150.9, 140.5, 102.7, 86.6, 83.5, 71.7, 70.9, 64.7, 59.1. ESI$^+$-MS: m/z 284.3 $[M + H]^+$.

5′-*O*-Methyl-2′-amino-2′-deoxyuridine (11)

5′-*O*-Methyl-2′-azido-2′-deoxyuridine (**10**, 1.33 g, 4.70 mmol) and triphenyl phosphine (2.46 g, 9.38 mmol) were dissolved in pyridine (4.7 mL). The mixture was stirred at 45 °C for 20 h, after which pyridine (47 mL) and concentrated aq. ammonia (47 mL) were added. The stirring was continued for 72 h, after which the reaction mixture was evaporated to dryness. The residue was purified on a silica gel column eluting with a mixture of MeOH and CH_2Cl_2 (15 : 85, v/v). Yield 0.98 g (81%). ^{1}H NMR (δ_H)(500 MHz, DMSO-d_6): 11.45 (s, 1H), 7.66 (d, 1H, J = 8.2 Hz), 5.69 (dd, 1H, J = 7.8 Hz), 5.67 (d, 1H, J = 8.2 Hz), 5.52 (s, 1H), 4.12 (s, 2H), 3.95 (ddd, 1H, J_1 = J_2 = 4.1 Hz, J_3 = 2.2 Hz), 3.87 (dd, 1H, J_1 = 5.3 Hz, J_2 = 1.9 Hz), 3.51 (dd, 1H, J = 10.6 Hz, J_2 = 4.0 Hz), 3.47 (dd, 1H, J_1 = 10.6 Hz, J_2 = 4.2 Hz), 3.31 (s, 3H), 3.29 (dd, 1H, J_1 = 7.9 Hz, J_2 = 2.5 Hz). ^{13}C NMR (δ_H)(125 MHz, DMSO-d_6): 163.5, 151.5, 141.0, 102.6, 88.3, 84.3, 73.1, 71.8, 59.1, 57.4. UV-VIS: λ = 260.0 nm, log(ε) = 4.02. HPLC: t_R = 6.8 min [Hypersil-Keystone Aquasil C18 column (4 × 150 mm, 5 μm); flow rate = 1 mL min^{-1}; 60 mM acetate buffer (pH = 4.3) and a linear gradient of 3→50% MeCN during 60 min, then 50% MeCN for 20 min]. HRMS (ESI$^+$): m/z calcd 258.1084 obsd 258.1074 $[M + H]^+$.

5′-*O*-Methyl-2′-trifluoroacetamido-2′-deoxyuridine (7)

5′-*O*-Methyl-2′-amino-2′-deoxyuridine (**15**, 0.96 g, 3.73 mmol) and *S*-ethyltrifluorothioacetate (0.73 mL, 4.62 mmol) were dissolved in MeOH (75 mL). The mixture was stirred at room temperature for 22 h, after which it was treated with N_2 for 10 min and evaporated to dryness. The residue was purified on a silica gel column eluting with a mixture of MeOH and CH_2Cl_2 (15 : 85, v/v). Yield 1.05 g (79%). ^{1}H NMR (δ_H)(500 MHz, DMSO-d_6): 11.37 (d, 1H, J = 3 Hz), 9.44 (d, 1H, J = 8.2 Hz), 7.74 (dd, 1H, J_1 = 8.1 Hz, J_2 = 1.4 Hz), 6.03 (d, 1H, J = 7.2 Hz), 5.85 (d, 1H, J = 5.0 Hz), 5.72 (d, 1H, J = 8.1 Hz), 4.49 (m, 1H), 4.17 (m, 1H), 4.03 (m, 1H), 3.58 (dd, 1H, J_1 = 11.0 Hz, J_2 = 3.4 Hz), 3.53 (dd, 1H, J_1 = 11.0 Hz, J_2 = 4.6 Hz), 3.35 (s, 3H). ^{13}C NMR (δ_H)(125 MHz, DMSO-d_6): 163.4, 151.1, 151.0, 140.9, 102.9, 86.2, 84.3, 72.6, 69.6, 59.1, 55.5. UV-VIS: λ = 260.0 nm, log(ε) = 4.08. HPLC: t_R = 15.9 min [Hypersil-Keystone Aquasil C18 column (4 × 150 mm, 5 μm); flow rate = 1 mL min^{-1}; 60 mM acetate buffer (pH = 4.3) and a linear gradient of 3→50% MeCN during 60 min, then 50% MeCN for 20 min]. ESI$^+$-MS: m/z 354.5 $[M + H]^+$.

N^6-Benzoyl-2′,3′-*O*-methyleneadenosin-5′-yl 5′-*O*-methyl-3′-*O*-(4,4′-dimethoxytrityl)uridin-2′-yl 5′-*O*-methyl-2′-trifluoroacetamido-2′-deoxyuridin-3′-yl phosphate (5b)

N^6-Benzoyl-2′,3′-*O*-methyleneadenosine (**6**, 0.85 g, 2.22 mmol) was coevaporated from anhydrous pyridine and dissolved in anhydrous MeCN under inert atmosphere. 1*H*-Tetrazole (0.186 g, 2.66 mmol) in anhydrous MeCN (5.9 mL) and tris(dimethylamino)phosphine (0.46 mL, 2.53 mmol) were added and the resulting mixture stirred at room temperature for 3 h. 5′-*O*-Methyl-2′-trifluoroacetamido-2′-deoxyuridine (**7**, 0.79 g, 2.24 mmol), 1*H*-tetrazole (0.186 g, 2.66 mmol) and anhydrous MeCN (5.9 mL) were added and the stirring was continued for 21 h. 5′-*O*-Methyl-3′-*O*-(4,4′-dimethoxytrityl)uridine (2.49 g, 4.44 mmol), 1*H*-tetrazole (0.186 g, 2.66 mmol) and anhydrous MeCN (5.9 mL) were added and the stirring was continued for 24 h. To one half of the reaction mixture (12.5 mL) was added a mixture of I_2 (0.5 g, 1.96 mmol), H_2O (8.55 mL), THF (17.15 mL) and 2,6-lutidine (4.3 mL). The resulting mixture was stirred at room temperature for 3 h, after which it was evaporated to dryness. The residue was partitioned between CH_2Cl_2 (100 mL) and 5% aq. $NaHCO_3$ (100 mL), the organic phase was evaporated to dryness and the residue was purified on a silica gel column eluting with a mixture of Et_3N, MeOH, CH_2Cl_2 and EtOAc (88 : 2 : 9 : 1, v/v). Yield 0.41 g (28%). ^{1}H NMR (δ_H)(500 MHz, DMSO-d_6): 11.49 (s, 1H), 11.38 (s, 1H), 11.21 (s, 1H), 8.72 (s, 1H), 8.65 (s, 1H), 7.82 (s, 1H), 7.71 (d, 1H, J = 8.2 Hz), 7.68–7.16 (m, 18H), 7.04 (d, 1H, J = 8.2 Hz), 6.34 (d, 1H, J = 2.7 Hz), 6.23 (d, 1H, J = 8.1 Hz), 6.13 (d, 1H, J = 8.3 Hz), 5.76 (dd, 1H, J_1 = 8.1 Hz, J_2 = 2.0 Hz), 5.43 (dd, 1H, J_1 = 6.6 Hz, J_2 = 2.7 Hz), 5.33 (dd, 1H, J_1 = 8.2 Hz, J_2 = 2.0 Hz), 5.22 (s, 1H), 5.21 (s, 1H), 5.02 (dd, 1H, J_1 = 6.5 Hz, J_2 = 4.3 Hz), 4.89 (m, 1H), 4.73 (m, 1H), 4.39 (m, 2H), 4.33 (m, 1H), 4.26 (m, 2H), 3.72 (s, 3H), 3.70 (s, 3H), 3.61 (dd, 1H, J_1 = 4.7 Hz, J_2 = 4.5 Hz), 3.47 (m, 1H), 3.40 (dd, 2H, J_1 = 10.9 Hz, J_2 = 3.1 Hz), 3.29 (dd, 2H, J_1 = 11.1 Hz, J_2 = 4.0 Hz), 3.16 (s, 3H), 3.14 (s, 3H). ^{31}P (δ_P)(202 MHz, DMSO-d_6): −2.41. ESI$^+$-MS: m/z 1342.5 [M + H]$^+$.

2′,3′-*O*-Methyleneadenosin-5′-yl 5′-*O*-methyl-3′-*O*-(4,4′-dimethoxytrityl)uridin-2′-yl 5′-*O*-methyl-2′-trifluoroacetamido-2′-deoxyuridin-3′-yl phosphate (4b)

N^6-Benzoyl-2′,3′-*O*-methyleneadenosin-5′-yl 5′-*O*-methyl-3′-*O*-(4,4′-dimethoxytrityl)uridin-2′-yl 5′-*O*-methyl-2′-trifluoroacetamido-2′-deoxyuridin-3′-yl phosphate (**5**, 70 mg, 0.052 mmol) was dissolved in saturated methanolic ammonia (35 mL). The mixture was stirred at room temperature for 6 h, after which it was evaporated to dryness. The crude product was purified by HPLC on a Supelcosil LC-18 column (25 cm × 21.2 mm, 12 μm) eluting with a mixture of MeCN and 0.05 mol L^{-1} aqueous NH_4OAc (44 : 56, v/v). Finally, the buffer salts were removed on the same column eluting with a mixture of MeCN and H_2O (50 : 50, v/v). Yield 38.1 mg (59%). ^{1}H NMR (δ_H)(500 MHz, DMSO-d_6): 8.32 (s, 1H), 8.15 (s, 1H), 7.70 (d, 1H, J = 8.2 Hz), 7.36–7.17 (m, 13H), 7.09 (d, 1H, J = 8.2 Hz), 6.19 (m, 3H), 5.73 (d, 1H, J = 8.1 Hz), 5.42 (d, 1H, J = 8.1 Hz), 5.34 (dd, 1H, J_1 = 6.5 Hz, J_2 = 2.9 Hz), 5.18 (s, 1H), 5.17 (s, 1H), 4.93 (dd, 1H, J_1 = 6.7 Hz, J_2 = 4.0 Hz), 4.90 (m, 1H), 4.68 (m, 1H), 4.35 (m, 2H), 4.28 (m, 1H), 4.23 (m, 2H), 3.72 (s, 3H), 3.70 (s, 3H), 3.58 (m, 2H), 3.37 (dd, 1H, J_1 = 11.3 Hz, J_2 = 3.6 Hz), 3.31 (dd, 2H, J_1 = 11.3 Hz, J_2 = 3.7 Hz), 3.19 (s, 3H), 3.15 (dd, 1H, J_1 = 11.2 Hz, J_2 = 2.5 Hz), 3.08 (dd, 1H, J_1 = 11.2 Hz, J_2 = 2.2 Hz), 3.12 (s, 3H). ^{31}P (δ_P)(202 MHz, DMSO-d_6): −2.38. UV-VIS: λ = 260.0 nm, log(ε) = 4.39. HPLC: t_R = 57.2 min [Hypersil-Keystone Aquasil C18 column (4 × 150 mm, 5 μm); flow rate = 1 mL min^{-1}; 60 mM acetate buffer (pH = 4.3) and a linear gradient of 3→50% MeCN during 60 min, then 50% MeCN for 20 min]. HRMS (ESI$^+$): m/z calcd 1237.3486 obsd 1237.3497 [M + H]$^+$.

Acknowledgements

Financial support from the Academy of Finland is gratefully recognized.

Notes and references

1 J. L. Hougland, R. N. Sengupta, Q. Dai, S. K. Deb and J. A. Piccirilli, *Biochemistry*, 2008, **47**, 7684; J. L. Hougland, S. K. Deb, D. Maric and J. A. Piccirilli, *J. Am. Chem. Soc.*, 2004, **126**, 13578; A. Yoshida, S. Shan, D. Herschlag and J. A. Piccirilli, *Chem. Biol.*, 2000, **7**, 85.
2 D. Herschlag, F. Eckstein and T. R. Cech, *Biochemistry*, 1993, **32**, 8312.
3 D. Herschlag and M. Khosla, *Biochemistry*, 1994, **33**, 5291.
4 T. Lönnberg and J. Korhonen, *J. Am. Chem. Soc.*, 2005, **127**, 7752.
5 T. Lönnberg, M. Ora, S. Virtanen and H. Lönnberg, *Chem.–Eur. J.*, 2007, **13**, 4614.
6 T. Lönnberg, J. Kiiski and S. Mikkola, *Org. Biomol. Chem.*, 2005, **3**, 1089.
7 S. A. Strobel and L. Ortoleva-Donnelly, *Chem. Biol.*, 1999, **6**, 153.
8 S.-O. Shan, A. Yoshida, S. Sun, J. A. Piccirilli and D. Herschlag, *Proc. Natl. Acad. Sci. U. S. A.*, 1999, **96**, 12299.
9 D. S. Knitt, G. J. Narlikar and D. Herschlag, *Biochemistry*, 1994, **33**, 13864.
10 S. Bakalova, W. Siebrand, A. Fernandez-Ramos, Z. Smedarchina and D. D. Petkov, *J. Phys. Chem. B*, 2002, **106**, 1476.
11 M. Forconi, R. N. Sengupta, M.-C. Liu, A. C. Sartorelli, J. A. Piccirilli and D. Herschlag, *Angew. Chem., Int. Ed.*, 2009, **48**, 7171; M. Guo, R. C. Spitale, R. Volpini, J. Krucinska, G. Cristalli, P. R. Carey and J. E. Wedekind, *J. Am. Chem. Soc.*, 2009, **131**, 12908; J. M. Thomas and D. M. Perrin, *J. Am. Chem. Soc.*, 2008, **130**, 15467; S. A. Strobel, *Nat. Chem. Biol.*, 2005, **1**, 5; S. R. Das and J. A. Piccirilli, *Nat. Chem. Biol.*, 2005, **1**, 45.
12 T. Lönnberg and S. Mikkola, *J. Org. Chem.*, 2004, **69**, 802.
13 M. Imazawa and F. Eckstein, *J. Org. Chem.*, 1979, **44**, 2039; W. A. Pieken, D. B. Olsen, F. Benseler, H. Aurup and F. Eckstein, *Science*, 1991, **253**, 314; J. P. H. Verheyden, D. Wagner and J. G. Moffatt, *J. Org. Chem.*, 1971, **36**, 250.
14 M. Kosonen and H. Lönnberg, *J. Chem. Soc., Perkin Trans. 2*, 1995, 1203.
15 M. Oivanen, M. Ora, H. Almer, R. Strömberg and H. Lönnberg, *J. Org. Chem.*, 1995, **60**, 5620.
16 H. S. Harned and B. B. Owen, *The Physical Chemistry of Electrolytic Solutions*, Reinhold Pub., New York, USA, 1958.
17 H. Åström, E. Limen and R. Strömberg, *J. Am. Chem. Soc.*, 2004, **126**, 14710.
18 J. Mullay, *J. Am. Chem. Soc.*, 1985, **107**, 7271.
19 N. Inamoto and S. Masuda, *Tetrahedron Lett.*, 1977, **18**, 3287; N. Inamoto, S. Masuda, K. Tori and Y. Yoshimura, *Tetrahedron Lett.*, 1978, **19**, 4547; N. Inamoto and S. Masuda, *Chem. Lett.*, 1982, 1007.
20 M. Kosonen, R. Seppänen, O. Wichmann and H. Lönnberg, *J. Chem. Soc., Perkin Trans. 2*, 1999, 2433; T. Lönnberg and H. Lönnberg, *Curr. Opin. Chem. Biol.*, 2005, **9**, 665.
21 R. Kluger and G. R. J. Thatcher, *J. Am. Chem. Soc.*, 1985, **107**, 6006; K. Taira, T. Fanni and D. G. Gorenstein, *J. Am. Chem. Soc.*, 1984, **106**, 1521; K. Taira and D. G. Gorenstein, *J. Org. Chem.*, 1984, **49**, 4531.
22 J. J. Stewart, *J. Mol. Model.*, 2007, **13**, 1173.
23 N. Bourne and A. Williams, *J. Org. Chem.*, 1984, **49**, 1200.

